Please check the marked (■) text passages carefully.

Stella Piovano

Gabriel L. Salierno

Emiliano Montmany

Mauro D'Agostino

Mauricio Maestri

Miryan Cassanello

LARSI, Dep. Industrias, FCEyN,
Universidad de Buenos Aires,
Buenos Aires, Argentina.

Bed Expansion and Particle Classification in Liquid Fluidized Beds with Structured Internals

The inclusion of a structured packing as internal in a liquid-solid fluidized bed allows expansion of the liquid velocity operation range before elutriation, promoting the liquid solid contact and mixing. The bed expansion of liquid-solid fluidized beds provided with structured packing as internals is examined, for solids denser than the liquid phase and within a wide range of operating conditions. A correlation to estimate the bed expansion in liquid-solid fluidized beds using structured packing as internals is developed. In addition, the feasibility of employing structured packing as internals for favoring classification of different density particles is demonstrated by analyzing the mass elutriated from the column at different liquid velocities for single particles or binary mixtures.

1 Introduction

Liquid-solid fluidization has gained increasing attention due to its potential application in several industrial fields, such as for biochemical processing, water and wastewater treatments, recycling of plastic materials from solid waste, food technology, among others. Additionally, the traditional use of liquid fluidization for mineral processing, particularly for separation of solids of different size and density, both at small and large scales, has continued for years [1–7].

Biochemical processes and wastewater biological treatments frequently involve aggregated and supported cells suspended in a liquid media, generally of high viscosity. The use of expanded solid-liquid suspensions allows homogenization of the cells, even if they are more subjected to shear than in a packed bed. Moreover, expanded bed adsorption or chromatography is now a well-established method for downstream processing of raw broths, allowing integration of the solid-liquid separation, volume reduction, and partial purification stages in one unit operation [8]. For expanded bed adsorption, it has been shown that the use of structured packing as internals leads to a more stable fluidization and extends the liquid operation range [9]. Cell growth has also been found to be more stable if the liquid-solid fluidized-bed reactor is supplied with a structured internal [10, 11]. Actually, biofilms can be grown on a static support through which the liquid or solid-liquid suspension circulates. Structured packings are appropriate supports for biofilm growth due to their high porosity and excellent mixing characteristics of the fluid phases [12]. Regular packings produce very low pressure drops due to their high void fraction and induce excellent contact between phases and good radial mixing [13, 14].

Bed expansion in liquid-solid fluidization depends on the liquid velocity and on the features of the suspended particles. For very small powders or light particles, bed expansion could be too large, and fines could be elutriated [2, 4]. Moreover, highly viscous liquids as those found in bioprocesses promote even larger bed expansions. Therefore, the maximum liquid velocity that can be employed without elutriation is limited. In this context, the use of regular packing as internals to extend the operational liquid velocity range and to simultaneously act as support for biofilms growth in case of wastewater treatments and biochemical processes in general, can be beneficial.

Bed expansion in liquid-solid fluidization has been extensively studied and characterized, particularly with the aim of understanding the phenomena [1, 3, 15]. However, the characteristics change notably when a structured packing is introduced in the bed as internal, and they have been only scarcely explored [9, 11, 16, 17].

Since bed expansion and particle elutriation depends on the features of the suspended particles, liquid fluidization has also been extensively applied for particle classification, especially in mineral processing [2, 4, 18–23]. Particularly complicated is the separation of fine particles of sizes less than 1 mm [24–28]. Moreover, in the last few years, much attention has been devoted to the use of inclined columns or inclined slits internals to promote the separation of particles [18, 19, 25–32].

Correspondence: Dr. Miryan Cassanello (miryan@di.fcen.uba.ar), Universidad de Buenos Aires, Facultad de Ciencias Exactas y Naturales, PINMATE, Departamento de Industrias, Intendente Güiraldes 2620, C1428BGA, Buenos Aires, Argentina.

© 2015 WILEY-VCH Verlag GmbH & Co. KGaA, Weinheim

In this context, the effect of using structured packing as internals on the bed expansion of a liquid-solid fluidized bed is examined. The expansion of liquid-solid fluidized beds with an incorporated regular packing is determined for a wide range of liquid velocities, with carboxymethyl cellulose (CMC) aqueous solutions of different viscosities. Suspended solid particles are alumina, sand, glass, and carbide, all of them denser than the liquid media. In addition, the capability of the structured packing for favoring particle classification is also explored. The mass of each kind of particles elutriated at different liquid velocities, while using single particles or binary mixtures of different density particles, is determined.

2   Experimental

The experimental setup contains acrylic columns of 1.5 m height and different diameters. The columns are fed with the solid particles from the bottom. A pump recirculates the model liquids used from a reservoir. Liquid flow rate is controlled by a diaphragm valve and measured with a flowmeter inserted in the circuit. The columns have Sulzer-type structured packings immediately above the solid feed zone. For experiments analyzing particle classification, elutriated solid is collected at the top of the column with a fine mesh sieve. Fig. 1 provides a scheme of the experimental setup and photographs of the internals used.
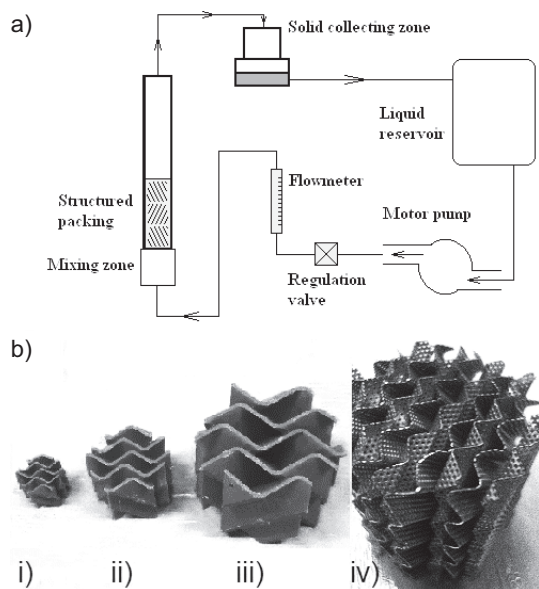
Figure 1. (a) Experimental setup; (b) photographs of the structured internals used: i) SP1, ii) SP2, iii) SP3; iv) SP4.

Bed expansion was measured by visual observation within a wide range of liquid velocities and using columns of different sizes and varying structured packing as internals. Several conditions were also examined with the empty column for comparison. Fluidized particles were alumina (A), sand (S), glass (G), and carbide (C), all of them denser than the liquid media. For nonspherical particles, a sphericity factor was determined from pressure drop measurements of the corresponding packed

beds. The liquid viscosity was varied from 1 to 23 mPa s using CMC aqueous solutions. CMC concentrations were low enough to ensure Newtonian rheological behavior of the liquid solutions. The range and some details of the explored experimental conditions are given in Tab. 1.

Table 1. Range of experimental conditions for bed expansion determination.

Variable	Conditions explored			
Column size, D_c [m]	0.016, 0.027, 0.044, 0.05			
Particle mean diameter, d_P [m]	0.000151, 0.000237, 0.000385, 0.000460, 0.000550			
Particle density [kg m^{-3}]	2460, 2590, 3140, 3815			
Particle sphericity, φ [–]	0.50, 0.59, 0.68, 0.81, 0.92, 1			
Mass of suspended particles [kg]	0.008, 0.020, 0.050, 0.1, 0.2, 0.3			
Structured packing characteristics	SP1	SP2	SP3	SP4
Void fraction, ε_{sp} [–]	0.768	0.759	0.814	0.950
External specific area, a_{sp} [m^{-1}]	176.9	123.8	65.9	734
Channel side length [m]	0.0038	0.0063	0.0105	0.0057
Liquid characteristics	Range [minimum – maximum]			
Liquid velocity, u_L [m s^{-1}]	0.001 – 0.05			
Liquid density, ρ_L [kg m^{-3}]	997 – 1005			
Liquid viscosity, μ_L [mPa s]	1 – 23			

Experiments aimed at examining the capability of the structured packing for favoring particle classification consisted in measuring the mass of solid elutriated from the column at different liquid velocities, both for single particles and for mixtures of particles of varying density. The liquid flow rate was progressively increased in steps of 20 L h^{-1}, corresponding to a superficial velocity of 0.003 m s^{-1}, at regular time intervals of 30 min. For each flow rate, the solid elutriated from the column during the 30-min intervals were collected at the column outlet. Samples of the solid mass taken during each interval were then observed and photographed by a digital microscope. The mass proportion on dry basis of the collected fractions was determined from the photos by image analysis. Tab. 2 indicates the conditions explored and the particles characteristics for each run.

3   Results and Discussion

3.1   Bed Expansion in Liquid-Solid Fluidized Beds with Internals

Bed expansions of the liquid-solid fluidized beds were examined for the wide range of conditions given in Tab. 1, and com-

Table 2. Solids employed for experiments to examine particle classification.

Run	Particle A [a]	Particle B [a]
I	–	G385(100 wt %)
II	A385(100 wt %)	–
III	A385(50 wt %)	G385(50 wt %)
IV	–	G460(100 wt %)
V	A460(100 wt %)	–
VI	A460(50 wt %)	G460(50 wt %)
VII [b]	–	G545(100 wt %)
VIII [b]	A545(100 wt %)	–
IX [b]	A545(50 wt %)	G545(50 wt %)

Alumina density: 3815 kg m^{-3}; glass density: 2460 kg m^{-3}; alumina sphericity: 0.7–0.9; glass sphericity: 0.9–1; column diameter: 0.05 m; liquid viscosity: 1 mPa s.

Structured packing characteristics (SP4): corrugated metal sheets, void fraction: 0.95; external specific area: 734 m^{-1}; channel side length: 0.0057 m; corrugation angle: 78°.

Mean diameters are defined considering the sieves used for getting the corresponding fraction

d_P = 385 μm corresponds to the fraction between 360 and 420 μm.
d_P = 460 μm corresponds to the fraction between 420 and 500 μm.
d_P = 545 μm corresponds to the fraction between 500 and 590 μm.

[a] Notation of suspended particles is symbolized by a letter indicating the material, followed with a number that gives the mean particle diameter in μm.
[b] Runs VII to IX have also been carried out in the empty column for comparison.

pared with the behavior of the corresponding empty columns. Fig. 2 shows the superficial liquid velocity required to expand the bed as a function of the attainable bed void fraction or liquid holdup. The figure illustrates the influence of employing structured packings as internals on the measured liquid holdup, for beds of single particles of the same size and different density, with water and a viscous liquid. The comparison with the behavior of empty columns evidences that the use of a structured packing as internal largely extends the liquid velocity range within which particles are suspended in the liquid before being elutriated. The effect of the internal becomes more important as the suspended particles holdup decreases, i.e., for the high porosity range. Both in the empty column and in the column provided with the internal, an increase of liquid viscosity promotes bed expansion.

Fig. 3 allows comparing the liquid holdup attained in liquid-solid fluidized beds of similar size provided with different structured packings as internals, for particles of similar size and different densities (A385 and S385), and particles of similar density and different sizes (G545 and S385). The influence of the structured packing used as internal on the bed expansion depends on the particles used, particularly for suspended par-
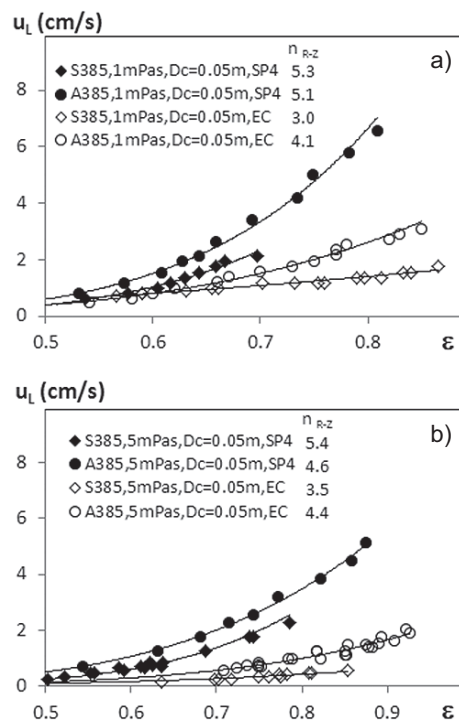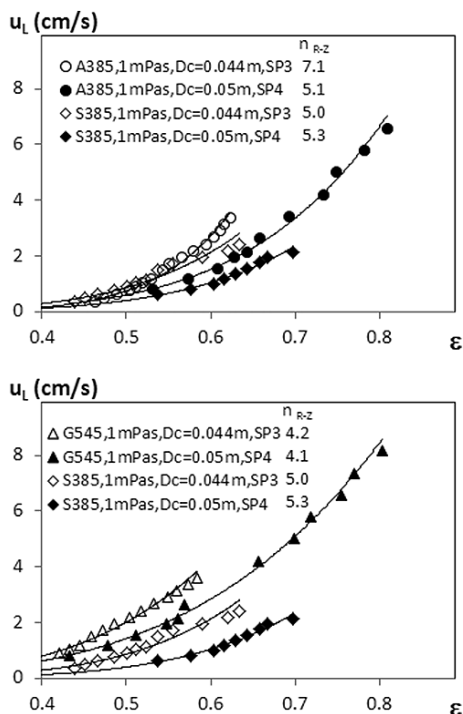

Figure 2. Comparison of the liquid holdup in a liquid-solid fluidized bed with and without a structured packing as internal. A385: alumina, d_P = 385 μm; S385: alumina, d_P = 385 μm. EC: empty column, SP4: column provided with a structured packing as internal. Column diameter is given in the legend. Liquid viscosity: (a) 1 mPa s, (b) 5 mPa s. Solid lines represent the fitting of the Richardson-Zaki expression with the exponents indicated in the legend.

ticles of the same size and different densities. When the corrugated metal sheet structured packing is applied, two distinct curves are observed for particles of different density, while the curves separate only after a given bed void fraction when using a Sulzer static mixer as internal. According to Fig. 4, the liquid viscosity does not modify essentially the effect of the type of internal used.

Bed expansion in empty columns has been extensively studied and general correlations are available to estimate the expansion of liquid-solid fluidized beds [15]. The widely used correlations of Wen and Yu [33] estimate satisfactorily experimental results of this work measured in the empty columns, considering a sphericity factor for nonspherical particles. However, correlations available in the literature for empty columns fail to estimate the measured liquid holdups when the column is provided with a structured packing as internal, even if the superficial liquid velocity is divided by the structured packing void fraction to calculate the dimensionless numbers involved in the correlations.

Data measured in the empty columns are properly represented by the well-known Richardson and Zaki [34] relation (Eq. (1)), with exponents in the range of 3 to 5. Terminal velocities of the particles used in the empty columns agree well with the correlation of Martin [35]. When introducing a structured internal in the column, both the terminal velocities and the
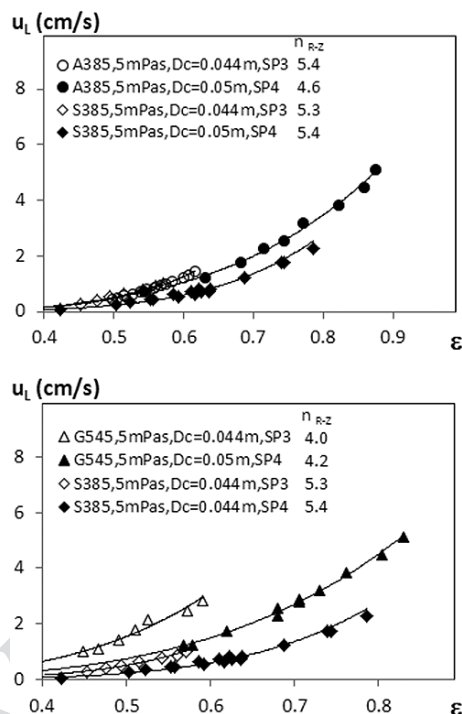
Figure 3. Comparison of the liquid holdup in liquid-solid fluidized beds with different structured packing as internals. SP3: plastic Sulzer static mixer, SP4: structured packing formed by a corrugated metal sheet. A385: alumina, $d_p = 385\,\mu m$, $\rho_p = 3815\,kg\,m^{-3}$; S385: sand, $d_p = 385\,\mu m$, $\rho_p = 2590\,kg\,m^{-3}$; G545: glass, $d_p = 545\,\mu m$, $\rho_p = 2460\,kg\,m^{-3}$. Column diameters are given in the legend. Liquid viscosity: 1 mPa s. Solid lines represent the fitting of the Richardson-Zaki expression with the exponents indicated in the legend.

Figure 4. Comparison of the liquid holdup in liquid-solid fluidized beds with different structured packing as internals. SP3: plastic Sulzer static mixer, SP4: structured packing formed by a corrugated metal sheet with orifices. A385: alumina, $d_p = 385\,\mu m$, $\rho_p = 3815\,kg\,m^{-3}$; S385: sand, $d_p = 385\,\mu m$, $\rho_p = 2590\,kg\,m^{-3}$; G545: glass, $d_p = 545\,\mu m$, $\rho_p = 2460\,kg\,m^{-3}$. Column diameters are given in the legend. Liquid viscosity: 5 mPa s. Solid lines represent the fitting of the Richardson-Zaki expression with the exponents indicated in the legend.

exponent n becomes larger than the one found for empty columns [36, 37]. Values of the exponent can even double those obtained for the empty columns, especially for the smaller and denser particles and highly viscous liquids. Fitted exponents are reported for the conditions mentioned in Figs. 2 to 4 in the legend, and the ability of the Richardson-Zaki [34] relation to fit the curves is also given for these representative conditions. In addition, Hicketier and Buchholz [9] found exponents larger than the ones predicted by the correlation of Richardson-Zaki [34] in a liquid-solid fluidized bed provided with a structured packing, used for purification of a protein by expanded bed adsorption.

$$\frac{u_L}{u_t} = \varepsilon^n \qquad (1)$$

where u_L[1]) is the liquid superficial velocity, u_t is the terminal liquid velocity, and ε is the void fraction.

Metzdorf et al. [11, 16, 17] also stated a similar trend of requiring significantly larger liquid velocities for attaining the same liquid-solid fluidized bed expansions while using struc-

tured internals. These authors reported a dimensional correlation to estimate bed voidage, based on the liquid superficial velocity, the hydraulic diameter of the internal used, and the liquid kinematic viscosity. There is no explicit influence of the particle size in the correlation, likely because the mean diameter of the particles used by the authors varied in a rather limited range of 100 to 200 μm. The correlation proposed by Metzdorf et al. [17] overestimates the bed void fraction measured in this work, particularly for the viscous fluids and for particles larger than 385 μm.

To develop a correlation based on the databank of around 1400 experiments measured with columns of varying diameters, provided with structured packings of different characteristics, using particles of diverse features and liquids of several viscosities, the expression of the correlation of Wen and Yu [33] was considered to represent the experimental results. Parameters were refitted after introducing a new dimensionless group to take into account the characteristics of the internal. The dimensionless group used in this case was selected as the ratio of the suspended particles mean diameter d_p, corrected by sphericity φ, to a hydraulic equivalent diameter, d_h. The hydraulic equivalent diameter was defined considering the porosity, ε_{sp}, and the specific area, a_{sp}, of the structured packing, as indicated in Eq. (2).

---

1)　List of symbols at the end of the paper.

$$d_{\mathrm{h}} = 4\varepsilon_{\mathrm{sp}}/a_{\mathrm{sp}} \qquad (2)$$

The correlation which best fits the experimental databank is given by Eq. (3). The ability of the current expression to estimate the experimental results for the whole databank is illustrated in Fig. 5.

The correlation estimates the experimental data with the standard deviation of 3.7 % and the variation coefficient of 6.4 %.

$$\varepsilon^{6.8} = \frac{(2.4Re_{\mathrm{L}} + 0.6Re_{\mathrm{L}}^2)}{Ar}\left(\frac{d_{\mathrm{p}}\phi}{d_{\mathrm{h}}}\right)^{0.23} \qquad (3)$$

3.2 Particle Classification Using Liquid-Solid Fluidized Beds with Internals

Since the last decade, a remarkable work has been developed for evidencing the strong influence of inclined slits internals on liquid-solid fluidized bed expansion [19, 30]. It was shown that the bed expansion can be decreased for a given liquid velocity by conveniently positioning inclined slits as internals within the fluidization region. Furthermore, based on this concept, successful applications towards particle classification were accomplished ([26–28, 31] among others). Moreover, recently, Hagemeier et al. [38] studied by simulation the separation efficiency of a pilot-scale zigzag apparatus for particle classification by flowing air.

The structured packing formed by corrugated metal sheets resembles inclined sheets that changes direction for each element. It has a strong influence on the bed expansion, which becomes more evident as the liquid holdup increases, and the influence is apparently more marked on denser particles, as can be observed in Fig. 2. Therefore, the ability of the column provided with a structured packing as internal on classification of different density particles was examined.
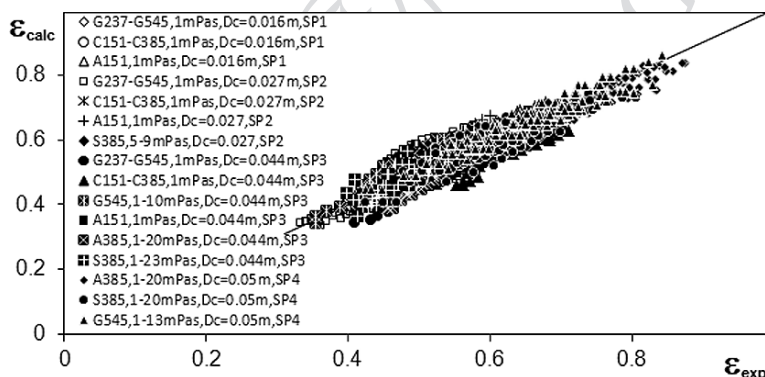
Figure 5. Experimental vs. predicted values of liquid holdup in liquid-solid fluidized beds of different size and with different structured packings as internals. Suspended particles are noted with a letter indicating the material, followed with a number that gives the mean particle diameter in µm. A: alumina, S: sand, G: glass, C: carbide. SP1, SP2, and SP3: plastic Sulzer-type static mixers of different diameters, SP4: structured packing of corrugated metal sheets. Liquid viscosity and column diameter are given in the legend.

With high liquid velocities, the suspended particles can be elutriated from the column. Fig. 6 illustrates the performance of the liquid-solid fluidized bed provided with SP4 as internal for separating particle mixtures of different densities. Mixtures of equal mass proportion of particles of the same size and different densities were fluidized and finally elutriated by increasing progressively the liquid velocity in regular steps of $0.003\,\mathrm{m\,s^{-1}}$. After each liquid flow rate increase, the mass leaving the column was collected during 30 min at the column outlet with a sieve of very fine mesh. The elutriated particles were then dried and weighed. The fraction of glass and alumina in the elutriated mass was then determined by image analysis from photographs taken with a digital microscope.

Fig. 6 presents the fraction of each particle elutriated from the column provided with SP4 during the considered time interval at different liquid velocities and for particles of three mean diameters. For the biggest particles used, the separation attained with the empty column is also indicated for comparison. Figs. 7 and 8 give the corresponding cumulated mass of each elutriated particle from the mixture and compare with the elutriated mass obtained when the single particles are fluidized.

Glass particles equal and larger than 460 µm (Figs. 6 b and c) leave the column almost free of denser alumina particles for a wide range of liquid velocities. Eventually, for liquid velocities larger than $0.08\,\mathrm{m\,s^{-1}}$, the alumina particles are also dragged out of the column by the circulating liquid. For liquid velocities between 0.08 and $0.1\,\mathrm{m\,s^{-1}}$, the mass fractions of both solid particles leaving the column are comparable, while for liquid velocities larger than $0.1\,\mathrm{m\,s^{-1}}$, only alumina particles remain in the column and are finally elutriated. This behavior suggests that operating at liquid velocities close to $0.08\,\mathrm{m\,s^{-1}}$ would allow recovering from the column a significant amount of the corresponding glass particles almost free of alumina. The mass fractions of a similar mixture elutriated from the empty column, indicated in Fig. 6 c, evidences the improvement in separation that can be attained simply by providing the column with a structured internal. Using the empty column, there is no liquid velocity leading to glass particles almost free of alumina ones.

Separation of small particles (Fig. 6 a) is less efficient. Despite a significant mass of glass particles can be recovered with less than 20 % alumina particles, no liquid velocity allows recovering glass particles free of alumina under the explored conditions. It is likely that the geometric characteristics of the structured packing used as internal would determine the minimum particle size which could be efficiently separated. This hypothesis still requires further experiments to be confirmed, and to establish criteria for choosing the best internal for improving particle separation with a liquid fluidized bed. In addition, supplementary experiments with continuous operation would allow establishing definitely the advantages of using structured internals for particle classification with a liquid fluidized bed.

The critical liquid velocity from which the particles start to leave the column depends on particle size for a given material; see Figs. 7 and 8. The larg-
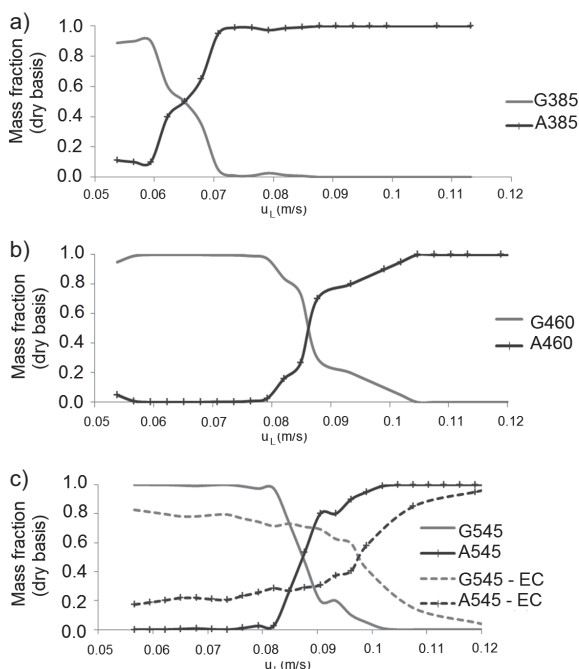
Figure 6. Mass fractions on dry basis of particles elutriated from the liquid-solid fluidized bed with SP4 as internal, at different liquid velocities. Runs (see Tab. 2): (a) III, (b) VI, and (c) IX and corresponding results in the empty column for comparison. Liquid viscosity: 1 mPa s. Composition of the elutriated mass determined by image analysis from digital pictures of the collected mass.
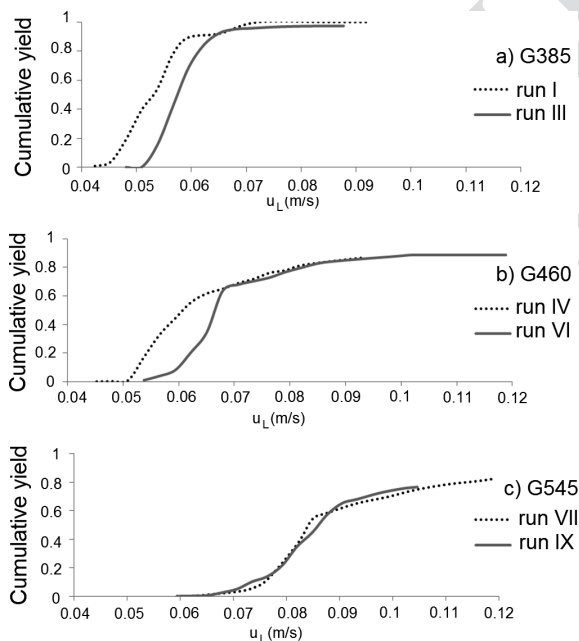
Figure 7. Cumulated mass fractions on dry basis of glass particles elutriated from the liquid-solid fluidized bed with SP4 as internal, at different liquid velocities. Comparison of elutriation curves while fluidizing single particles (runs I, IV, and VII, dashed lines) or binary mixtures (runs III, VI, and IX, solid lines). For run conditions see Tab. 2. Liquid viscosity: 1 mPa s.
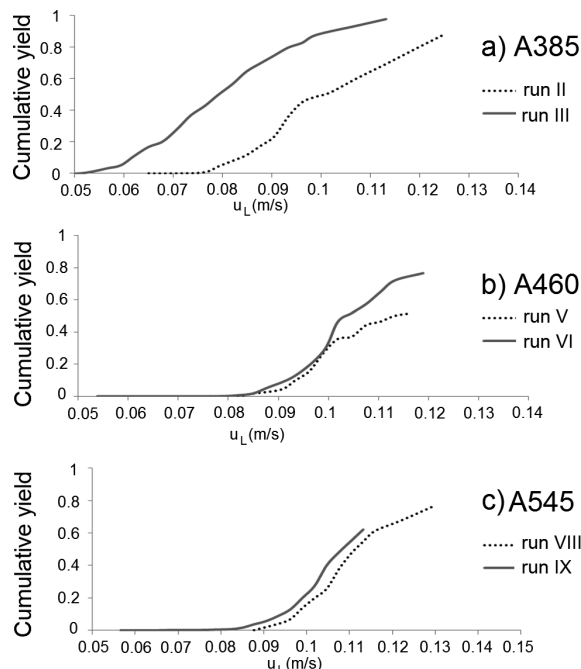
Figure 8. Cumulated mass fractions on dry basis of alumina particles elutriated from the liquid-solid fluidized bed with SP4 as internal, at different liquid velocities. Comparison of elutriation curves while fluidizing single particles (runs II, V, and VIII, dashed lines) or binary mixtures (runs III, VI, and IX, solid lines). For run conditions see Tab. 2. Liquid viscosity: 1 mPa s.

er the particle size, the higher the liquid velocity at which the particles start to be elutriated. These figures also highlight that the velocities at which given particles start to leave the column from a fluidized bed of single particles can be different than those found for binary mixtures, clearly indicating a strong interaction among particles of different classes. This behavior is not observed for the heavier particles, i.e., G545, A460, and A545, for which the cumulated elutriated mass is similar either from beds of single particles or mixtures.

Particles smaller than 460 μm interact strongly. When G385 particles are in a mixture, they start to leave the column at liquid velocities of 0.051 m s^{-1}, while they start to be elutriated at 0.042 m s^{-1} when there are only glass particles in the column (Fig. 7 a). This behavior is also observed for the G460 particles (Fig. 7 b). On the contrary, denser alumina particles (A385) are elutriated from a mixture at lower liquid velocities than from a fluidized bed of single particles (Fig. 8 a), indicating a positive drag of the glass particles exerted on the alumina ones for small particles. The cumulative elutriated mass curves of particles larger than 460 μm are similar for fluidized beds of single particles or for mixtures (Figs. 7 c and 8 c), indicating less interaction between the particles forming the mixtures.

A successful particle separation from a binary mixture can be achieved when the interaction between particles of different kind is weak enough. Moreover, the larger the difference between the liquid velocities at which each particle starts to be elutriated, the better the separation achieved. To quantify the separation efficiency, a parameter calculated as expressed in

Eq. (4) was considered, following the definition of resolution for a separation by chromatography [39].

$$\theta = \frac{u_{L_{r,A}} - u_{L_{r,G}}}{\sigma_A + \sigma_G} \qquad (4)$$

Where u_{L_r} indicates the liquid velocity for which each type of particle starts to leave the column from the fluidized binary mixture, called incipient elutriation. The parameters σ_A and σ_G quantify the width of the most significant peak of mass collection of each particle type, i.e., alumina and glass particles, respectively. The difference between the liquid velocity for which an inflection is observed in the cumulative yield and the liquid velocity at incipient elutriation has been considered as estimations of σ, for calculating θ.

The evolution of the resolution parameter defined in Eq. (4) is illustrated in Fig. 9 as a function of the particle size. In addition, the parameter calculated for the empty column for the bigger particles is also included for comparison. The defined parameter allows quantifying the classification capability of the fluidized bed and will be used for analyzing the effect of different internals on particle classification in future works.
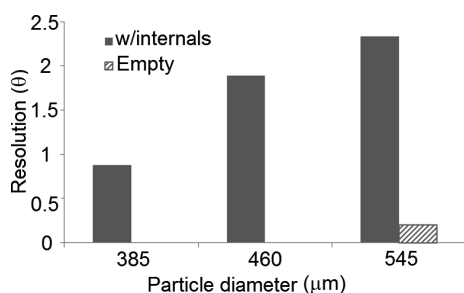
Figure 9. Influence of the particle size on the classification capability of the fluidized bed with SP4, from binary mixtures of particles of different densities, as evaluated with the parameter defined in Eq. (4). Comparison with the resolution in the empty column for the biggest particles examined.

4 Conclusions

The use of structured packing as internal in liquid-solid fluidized beds significantly decreases the bed expansion for a given liquid superficial velocity; thus, the structured internals are suitable for extending the operational liquid velocity range. The effect is especially observed for high-viscosity liquids, as those generally found for instance in bioprocesses. A correlation to estimate the liquid holdup in a liquid-solid fluidized bed provided with a structured packing as internal is developed. The proposed correlation is able to estimate the around 1400 databanks with the standard deviation of 3.7 % and the variation coefficient of 6.4 %.

Particle classification from mixtures of different density particles in a liquid-solid fluidized bed can be improved by using structured packing as internal. The improvement attained depends on the particle size. A parameter for quantifying the efficiency of a liquid-solid fluidized bed to separate particles forming a binary mixture has been introduced.

Acknowledgment

Symbols used

Ar	[–]	Archimedes number: $d_p^3 \rho_L (\rho_P - \rho_L) g / \mu_L^2$
a_{sp}	[m^{-1}]	specific external area of the structured packing
D_c	[m]	column diameter
d_p	[m]	particle mean diameter
d_h	[m]	hydraulic diameter defined in Eq. (2)
g	[m s^{-2}]	gravity acceleration
n	[–]	exponent of the void fraction in Eq. (1)
Re_L	[–]	liquid Reynolds number: $\rho_L u_L d_p / \mu_L$
u_L	[m s^{-1}]	liquid superficial velocity
u_{L_r}	[m s^{-1}]	liquid superficial velocity for incipient elutriation
u_t	[m s^{-1}]	terminal liquid velocity

Greek letters

ε	[–]	void fraction
ε_{sp}	[–]	porosity of the structured packing
μ	[Pa s]	viscosity
φ	[–]	sphericity factor
δ	[kg m^{-3}]	Density
σ	[m s^{-1}]	width in velocity units of the most significant peak of mass collection

Subscripts

A	alumina
G	glass
L	liquid
p	particle

References

[1] N. Epstein, in *Handbook of Fluidization and Fluid-Particle Systems* (Ed: W.-C. Yang), Marcel Dekker, New York **2003**.

[2] N. Epstein, *Powder Technol.* **2005**, *151 (1–3)*, 2–14. DOI: 10.1016/j.powtec.2004.11.026

[3] R. Di Felice, *Chin. Particuol.* **2007**, *5 (5)*, 312–320. DOI: 10.1016/j.cpart.2007.06.001

[4] R. Di Felice, *Basin Res.* **2010**, *22 (4)*, 591–602. DOI: 10.1111/j.1365-2117.2010.00460.xN

[5] N. Chowdhury, J. Zhu, G. Nakhla, A. Patel, M. Islam, *Chem. Eng. Technol.* **2009**, *32 (3)*, 364–372. DOI: 10.1002/ceat.200800564

[6] Y. Tatemoto, T. Michikoshi, T. Higashino, S. Maeda, S. Maeda, Y. Bando, *Chem. Eng. Technol.* **2012**, *35 (10)*, 1–8. DOI: 10.1002/ceat.201200201

[7] A. Atta, S. A. Razzak, K. D. P. Nigam, J.-X. Zhu, *Ind. Eng. Chem. Res.* **2009**, *48 (17)*, 7876–7892.

[8] F. B. Anspach, D. Curbelo, R. Hartmann, G. Garke, W.-D. Deckwer, *J. Chromatogr. A* **1999**, *865 (1–2)*, 129–144. DOI: 10.1016/S0021-9673(99)01119-X

[9] M. Hicketier, K. Buchholz, *J. Biotechnol.* **2002**, *93 (3)*, 253–268. DOI: 10.1016/s0168-1656(01)00408-4

[10] X. Z. Li, B. Hauer, B. Rosche, *J. Microbiol. Biotechnol.* **2013**, *23 (2)*, 195–204. DOI: 10.4014/jmb.1207.07057

[11] C. Metzdorf, P.-F. Fuquex, E. Flaschel, A. Renken, *Conserv. Recycl.* **1985**, *8 (1–2)*, 165–171. DOI: 10.1016/0361-3658(85)90033-5

[12] B. Rosche, X. Z. Li, B. Hauer, A. Schmid, K. Buehler, *Trends Biotechnol.* **2009**, *27 (11)*, 636–643. DOI: 10.1016/j.tibtech.2009.08.001

[13] O. N. Cavatorta, A. Chiappori, U. Böhm, *AIChE J.* **1999**, *45 (5)*, 938–948. DOI: 10.1002/aic.690450504

[14] O. N. Cavatorta, U. Böhm, *Chem. Eng. Technol.* **2000**, *23 (11)*, 1021–1026. DOI: 10.1002/1521-4125(200011)23:11<1021::AID-CEAT1021>3.0.CO;2-M

[15] R. Di Felice, *Chem. Eng. Sci.* **1995**, *50 (8)*, 1213–1245. DOI: 10.1016/0009-2509(95)98838-6

[16] C. Metzdorf, P. Fauquex, E. Flaschel, A. Renken, *German Chem. Eng.* **1985**, *8 (6)*, 358–361.

[17] C. Metzdorf, P. C. Singh, E. Flaschel, A. Renken, *Chem. Eng. Commun.* **1991**, *106*, 43–55. DOI: 10.1080/00986449108911534

[18] G. Nguyentranlam, K. P. Galvin, *Miner. Eng.* **2001**, *14 (9)*, 1081–1091. DOI: 10.1016/s0892-6875(01)00113-3

[19] K. P. Galvin, G. Nguyentranlam, *Chem. Eng. Sci.* **2002**, *57 (7)*, 1231–1234. DOI: 10.1016/s0009-2509(02)00005-2

[20] M. Duris, R. Garic-Grulovic, Z. Arsenijevic, D. Jaćimovski, Z. Grbavcic, *Powder Technol.* **2013**, *235*, 173–179. DOI: 10.1016/j.powtec.2012.10.004

[21] A. K. Mukherjee, S. N. Gurulaxmi, *Miner. Process. Extr. Metall. Rev.* **2013**, *34*, 130–138. DOI: 10.1080/08827508.2011.635734

[22] Y. Tatemoto, A. Ishii, Y. Suzuki, T. Higashino, *Chem. Eng. Technol.* **2010**, *33 (7)*, 1169–1176. DOI: 10.1002/ceat.201000027

[23] Y. Tatemoto, T. Higashino, Y. Suzuki, T. Michikoshi, S. Maeda, Y. Bando, *Chem. Eng. Technol.* **2011**, *34 (6)*, 877–885. DOI: 10.1002/ceat.201100012

[24] B. Sarkar, A. Das, S. P. Mehrotra, *Int. J. Miner. Process.* **2008**, *86*, 40–49.

[25] A. K. Mukherjee, B. K. Mishra, R. V. Kumar, *Int. J. Miner. Process.* **2009**, *92*, 67–73. DOI: 10.1016/j.minpro.2009.02.011

[26] K. P. Galvin, J. Zhou, K. Walton, *Chem. Eng. Sci.* **2009**, *64 (9)*, 2003–2010. DOI: 10.1016/j.ces.2009.01.031

[27] K. P. Galvin, K. Walton, J. Zhou, *Miner. Eng.* **2010**, *23 (4)*, 326–338. DOI: 10.1016/j.mineng.2009.09.015

[28] K. P. Galvin, J. Zhou, J. E. Dickinson, H. Ramadhani, *Miner. Eng.* **2012**, *39*, 9–18. DOI: 10.1016/j.mineng.2012.06.013

[29] G. Nguyentranlam, K. P. Galvin, *Int. J. Miner. Process.* **2004**, *73 (2–4)*, 83–89. DOI: 10.1016/s0301-7516(03)00065-6

[30] E. Doroodchi, D. F. Fletcher, K. P. Galvin, *Chem. Eng. Sci.* **2004**, *59 (17)*, 3559–3567. DOI: 10.1016/j.ces.2004.05.020

[31] E. Doroodchi, J. Zhou, D. F. Fletcher, K. P. Galvin, *Miner. Eng.* **2006**, *19 (2)*, 162–171. DOI: 10.1016/j.mineng.2005.08.001

[32] D. Laskovski, P. Duncan, P. Stevenson, J. Zhou, K. P. Galvin, *Chem. Eng. Sci.* **2006**, *61 (22)*, 7269–7278. DOI: 10.1016/j.ces.2006.08.024

[33] C. Y. Wen, Y. H. Yu, *Chem. Eng. Prog. Symp. Ser.* **1966**, *62*, 100–111.

[34] J. F. Richardson, W. N. Zaki, *Trans. Inst. Chem. Eng.* **1954**, *32*, 35–53. DOI: 10.1016/s0263-8762(97)80006-8

[35] H. Martin, *Chem. Ing. Tech.* **1980**, *52*, 199–209. DOI: 10.1002/cite.330520303

[36] P. Delgado, *Eng. Thesis*, Universidad de Buenos Aires, Argentina **2005**.

[37] M. D'Agostino, *Eng. Thesis*, Universidad de Buenos Aires, Argentina **2010**.

[38] T. Hagemeier, H. Glöckner, C. Roloff, D. Thévenin, J. Tomas, *Chem. Eng. Technol.* **2014**, *37 (5)*, 879–887. DOI: 10.1002/ceat.201300670

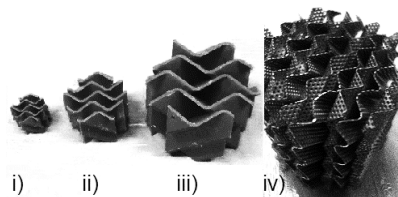[39] D. Forciniti, *Industrial Bioseparations: Principles and Practice*, 1st ed., Wiley-Blackwell, Oxford **2008**.

Research Article: A liquid-solid fluidized with internal allows extending the liquid velocity operation range before elutriation. A correlation to estimate the bed expansion in liquid-solid fluidized beds using structured packing as internals is proposed. Structured packing as internal in a liquid fluidized bed significantly favors classification of particles by density.

Bed Expansion and Particle Classification in Liquid Fluidized Beds with Structured Internals

S. Piovano, G. L. Salierno, E. Montmany, M. D'Agostino, M. Maestri, M. Cassanello*

i)   ii)   iii)   iv)